




Visual Analysis of Point Cloud Neighborhoods via Multi-Scale Geometric Measures

M. Ritter^{1,3} , D. Schiffner²  and M. Harders¹ 

¹Interactive Graphics and Simulation Group at the Department of Computer Science, University of Innsbruck, Austria

²DIPF | Leibniz Institute for Research and Information Education, Frankfurt, Germany

³Airborne Hydromapping GmbH, Innsbruck, Austria

Abstract

Point sets are a widely used spatial data structure in computational and observational domains, e.g. in physics particle simulations, computer graphics or remote sensing. Algorithms typically operate in local neighborhoods of point sets, for computing physical states, surface reconstructions, etc. We present a visualization technique based on multi-scale geometric features of such point clouds. We explore properties of different choices on the underlying weighted co-variance neighborhood descriptor, illustrated on different point set geometries and for varying noise levels. The impact of different weighting functions and tensor centroids, as well as point set features and noise levels becomes visible in the rotation-invariant feature images. We compare to a curvature based scale space visualization method and, finally, show how features in real-world LiDAR data can be inspected by images created with our approach in an interactive tool. In contrast to the curvature based approach, with our method line structures are highlighted over growing scales, with clear border regions to planar or spherical geometric structures.

CCS Concepts

• **Human-centered computing** → **Visual analytics**; • **Computing methodologies** → **Point-based models**;

1. Introduction

Point sets are commonly employed as a geometrical data structure, generated e.g. based on sensor or simulation data. Another use is in the context of object classification or object synthesis; there, point sets enhance labelled images and/or object models [MGY*19]. In any case, local neighborhood information is an essential component in many point based algorithms; and even more so when including point set hierarchies. Similar to the latter, multi-scale views can be employed, for instance in tensor based algorithms dealing with geometry processing on surfaces; e.g. to close holes or to denoise meshes [LCZ*18, WLP*17]. Related to this, we also employ a multi-scale view on local neighborhoods providing a geometric classification. Specifically, we are interested in reconstruction of line structures from noisy points clouds, and in the selection of optimal neighborhood sizes for this. Our introduced feature images allow to evaluate for optimal bandwidths and to visualize the effect of parameter choices in the underlying co-variance analysis.

Our contributions in short are:

- Multi-scale feature images based on a weighted co-variance measure to visualize linear, planar, and spherical structures.
- Visual analysis of different point set properties; such as shape and noise. Especially, the linearity measure was used for an optimal bandwidth selection with the related Eigenvector.
- Investigation of different weighting functions and centroids employed in the co-variance, optimized for visualization.

- Integration into an intuitive visual analysis tool.

Related to our work, Mellado et al. [MGB*12] introduced a continuous, multi-scale space based parameter derived from geometric properties of a fitted sphere on a cloud's points. The parameters relate to an algebraic fit, and include curvature, a distance, and the sum of distances (fitness). They show a similar visualization of the scale space which includes positive and negative curvature. For this, they require normal vectors at the points. Further, they provide a scale space image based on co-variance, as introduced by Pauly et al. [PKG03]. They utilize this visualization to represent curvature, which has a similar appearance as our visualization. They continued their research in the direction of surface reconstruction, and employ the curvature scale space for point segmentation and developed an interactive tool for geometric surface classification [LMBM20].

Further, Amirkhanov et al. [AHK*13] use a similar visualization technique to reveal surface probabilities of a material interface, over multiple scales at selected edges. Their selection relates to the line probes presented here. They enable to inspect ground truth shapes w.r.t. the scanned surface. Three graphs are provided for visual inspection, denoting straightness, flatness, and circularity. In contrast, in our method no reference geometry is required; and the line probe is not directly included in the geometrical analysis, but rather defines a region of interest. Their three measures relate to the shape factors, but are shown independently. While this reveals

related details, our measures provide a quicker overview. Further, our work is tailored to point clouds in contrast to their voxel based surfaces.

Regarding our geometric measures we follow Westin et al. [WPG*97], who employed tensor shape analysis for fiber tracking in the human brain. Natale et al. [NBT10] applied the same shape factors on point clouds, which they obtained from time-of-flight images. They introduced a decision network based on multi-scale shape values at different scales. The latter permitted them to classify a point as being part of a planar, edge/linear structure or as noise. We also built upon this multi-scale idea and developed a visualization technique to reveal properties of the tensor computation as well as the point cloud neighborhoods, via color-mapped images. In the tensor computation we employ radial distance weighting functions, which we also analyze visually. For these, several different choices are possible; for instance, SPH smoothing kernels or compactly supported radial distance functions and their recent optimizations, e.g. [CS20].

2. Geometric Analysis via Local Shape Measures

Shape factors: Local geometric measures are computed via a weighted co-variance analysis. The tensor's eigenvalues yield three shape factors: linearity, planarity, and sphericity [WPG*97]:

$$\mathbf{t} = \frac{1}{\sum_{i=1}^N \omega(d_i)} \sum_{i=1}^N \omega(d_i) (v_i \otimes v_i), \quad \text{with} \quad (1)$$

$$v_i = p_i - c, \quad d_i = |v_i|/r, \quad \text{yielding}$$

$$C_L = (\lambda_3 - \lambda_2)/L, \quad C_P = 2(\lambda_2 - \lambda_1)/L, \quad C_S = 3\lambda_1/L, \quad (2)$$

with \mathbf{t} the second order tensor, c a point of reference (i.e. the *centroid*), p_i the neighbors, $\omega(\cdot)$ a distance weighting function, and r a radius of the local neighborhood of interest. The three shape-factors C_L , C_P , and C_S are computed from the eigenvalues λ_i of \mathbf{t} ; with $L = \lambda_0 + \lambda_1 + \lambda_2$. They span a barycentric coordinate system; thus, three colors can be assigned and interpolated: e.g. bright gray (linearity), dark blue (planarity), and medium green (sphericity).

Multi-scale view: Eq. (1) initially relies on a specific fixed neighborhood radius which can be difficult to specify for an arbitrary point cloud. Instead, we propose to change this radius over multiple scales. The step size is automatically chosen based on a minimum distance statistic of the points cloud (the median radius of all neighborhoods comprising of at least 6 neighbors). The growth can be terminated e.g. dependent on the difference to the features of the previous scale. If it becomes small for all points, the iteration is stopped early. Figure 1 illustrates how the three shape factors change, as functions of the radius. The graphs were determined for a specific centroid, in a point set representing a square. As can be seen, the linearity graph decreases, when the radius grows to include the corner; at this point, planarity starts to increase. For a more compact representation, the three scalar graphs (and base colors) can be merged into mixed colors, which is indicated by a color-bar in the bottom of the figure. Such color-bars are computed for a specific location and represent the change of the shape factors with changing radii. Differences in these color-bars will result, dependent on point cloud location. These bars are assembled next to each other for neighboring points of a point set. Figure 2

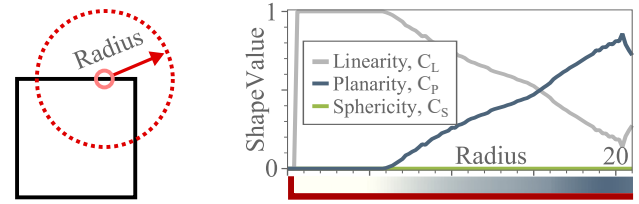


Figure 1: Geometric measures (right) computed for a centroid location in an example point cloud of a square (left). Resulting geometric measures depend on the selected radius; linearity in the example is initially high and decreases when a corner is reached. The color bar (right, bottom) indicates the barycentric mixing of the three base colors (in the 2D example only blue and light-gray).

shows an example of such a visualization, for the point cloud of a square. Note that the abscissa denotes the (ordered) point index, while the ordinate represents the increasing radius. The corners in the square are dominant with respect to planarity (blue); the edges are dominant with respect to linearity (light-gray). Thus, the assembled color-bars provide insight into the dominant shape features at various scales. We denote these images as multi-scale feature images (MSFIs). Note that in arbitrary point clouds, points are not necessarily ordered (as for the artificial square example). Still, an ordering could be achieved, e.g. by sorting locally along the major eigenvector of a selected point of reference. Another option could be sorting along a path provided by a user (see below).

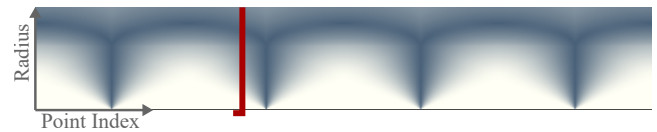


Figure 2: This multi-scale feature image (MSFI) illustrates the geometric measures by mixing the base colors; pixel columns (vertically) denote a single measure graph at a specific location, for varying radii. The red line marks the geometric measures for the point on the square in Figure 1.

3. Analysis of the Visualization Method

In this section we first provide an investigation of the proposed visualization approach on simple 2D and 3D geometries. We also present a visual analysis of the influence of weighting functions and chosen centroids for the tensor computation.

Test geometries: For simplicity, we visualize the multi-scale features of four 2D and two 3D sampled point clouds. Figure 3 shows the resulting, rotation-invariant MSFIs. Various geometric properties can be seen, e.g. corners (planar/spherical peaks), straight lines (bright areas), and curvature in and out of a plane (fading from light-gray). Three of the geometries will be used for further discussion and analysis below: rectangle (a), helix (b), 3D crossing (c).

Influence of tensor weighting: The weighting function $\omega(\cdot)$ in Eq. (1) influences the eigenvalue computation and thus the three measure graphs. As a result, the location of extrema in the graphs may change, as well as the graph shape. During our development, we investigated 30 different options for the weighting functions,

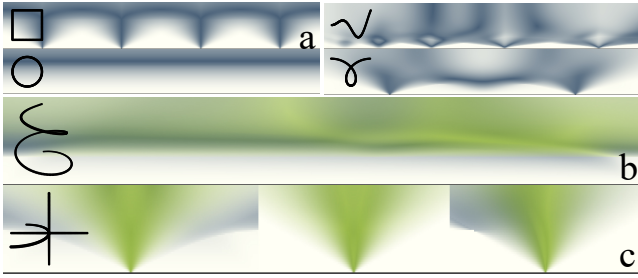


Figure 3: Geometric measures illustrated via MSFIs, of four 2D and two 3D point clouds of curves. Respective geometries are indicated on the left of the measure image. Geometric properties, such as corners, lines passing close-by, curvature, as well as 2D & 3D distribution become visible in the images.

and also explored the effect on the visualization. Figure 4 illustrates the outcome of different choices of $\omega(\cdot)$ on the linearity graph. Three weighting functions are examined: no weighting ω_0 , a quadratic weighting ω_2 , and a Fermi-Dirac distribution weighting ω_{FD} . In general, in combination with different centroids (see discussion below) a smoother weighting graph results in cleaner MSFIs. Nevertheless, having extrema located at smaller radii is preferable, since this saves computational cost in the neighborhood search. The MSFIs illustrated in this work all employ the Fermi-Dirac weighting, which showed the best performance related to line reconstructions in noisy point clouds.

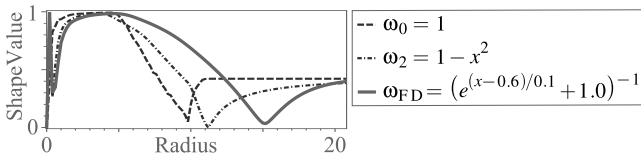


Figure 4: Influence of weighting functions on the multi-scale features, for jitter-noise data. Three of thirty functions are highlighted showing different minima locations and smoothness in linearity.

Centroid selection: Another choice in Eq. (1) is the centroid c . One could select an existing point of the point cloud, yielding the point distribution tensor (PDT); or compute a mean point (*mean*), yielding a standard co-variance matrix for principal component analysis; or select a geometric median instead (*median*). For the latter two, a new centroid has to be computed at each radius scale. The influence of these different choices also becomes apparent in the MSFIs; for instance, for the mentioned three test cases, now with added noise (see Figure 5). The *mean* and *median* result in more prominent shape regions, with clearer borders.

Influence of noise: Any noise present in a point cloud can also be scrutinized in the MSFIs (as shown in Figure 5). In the depicted example, perturbation noise with an amplitude of about 0.28 was added to the geometries (diameters of about 10.0), as well as 10% outliers within their bounding boxes. Examining the MSFIs, a horizontal green band results at a radius matching the amplitude (i.e. point distortion distance) of the added noise. Further, using the mean or geometric median as the centroid leads to better compensation of noise. Next, dependent on the light-gray regions reasonable bandwidths for line structures can be determined. Finally, as can

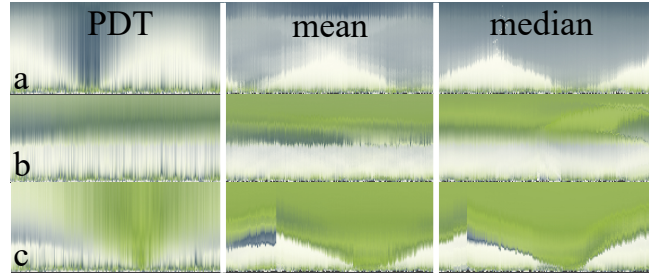


Figure 5: Effect of different centroids on visualizing noisy point neighborhoods on the geometries (a), (b), and (c) of Figure 3. Data was distorted by adding a random displacement. Mean and median centroids compensate for noise in the geometric measures.

be seen, dependent on the geometry, the optimal radius may vary; e.g. close to corners small radii are preferable, while in noisy data larger radii compensate noise.

4. Comparison and Application

Comparison: Using the framework of Mellado et al. [MLGB20, MGB*12] we generated the different scale space visualizations for comparison, compiled in Figure 6. Our visualization shows the shape factors, while theirs is based on curvature. Note that for the latter the required normal vectors were computed in our framework; by analyzing, selecting, and finally orienting the medium eigenvector. The three geometries (a), (b), and (c) are compared; for the first two, with and without noise. Both methods show straight lines as gray or white regions, i.e. linearity for our and zero curvature for their method (nevertheless, note that zero curvature would also result for a plane). As example, similar appearance can be seen for the rectangle (a) at the linearity scales (i.e. white for zero curvature). Next, the noise amplitude can in general also be detected in both; however, our measures distinguish better between 2D and 3D noise (green/blue coloring). In addition, the region boundaries are visually stronger, areas more homogeneous, and noise is better filtered. For the helix (b), the higher curvature region (darker red) can be matched with the linear one in our images. However, curvature differences become less apparent with added noise (right). Thus, the selection of a prominent linearity radius would become difficult using their visualization only. In our method smaller radii in the brighter band would be favored, whereas this is not visible in the lower radii band in their method. The 3D crossing (c) shows positive (red) and negative curvature (blue) at the curved lines. Our method classifies this region “just” as linear. Finally, in their method it is not straightforward to identify and segment the same regions, as borders are less prominent (left).

Application example: We have integrated the proposed visualization technique into an interactive framework for analysis of real-world point cloud data, captured by laser scanning. A central interaction element is a tool to allow users to define *line probes*. These are manually placed, polygonal lines, along which the geometric measures can be computed and visualized as MSFIs. Figure 7 showcases an example data set, comprising a house, a tree, and several cables. In the depictions (at the top), individual points in the cloud are colored according to the most prominent shape

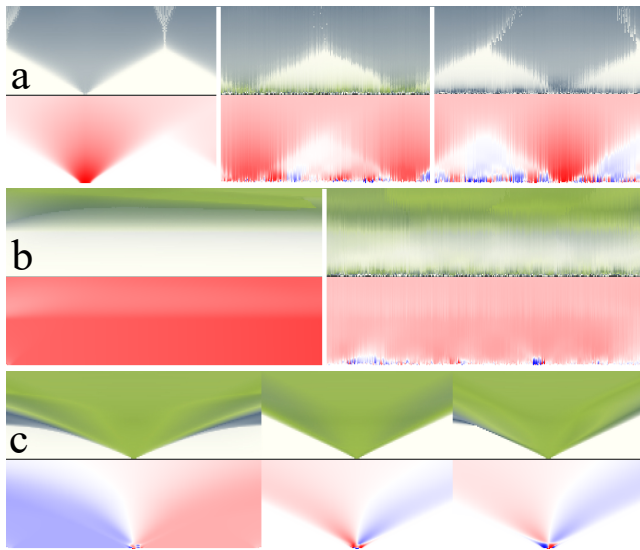


Figure 6: Images generated for rectangle (a), helix (b), and crossing 3D (c), based on our method as well as multi scale curvature using Mellado et al. [MGB*12]. Images are shown as pairs – ours above, theirs below, respectively. With our method 2D and 3D noise at small radii becomes distinguishable ((a); center/right). Further, linear regions are highlighted clearer ((b) and (c); left). Also, a band of smaller radii is highlighted in our images, but not visible according to curvature ((b); right). Finally, geometric classification is not clear based on curvature alone.

factor of the multi-scale measures. Two line probes were placed by a user into the cloud, and the corresponding multi-scale measures were computed and MSFIs generated along these. Different local features become apparent in the latter; (1) probe diagonally across the roof: planarity is prominent. Sphericity increases close to the gable (left); (2) a probe located on the top one of a bundle of cables, to the right of the house: linearity is dominant at two scales; firstly, at a very small scale for the single cable and secondly, for the bundle of cables.

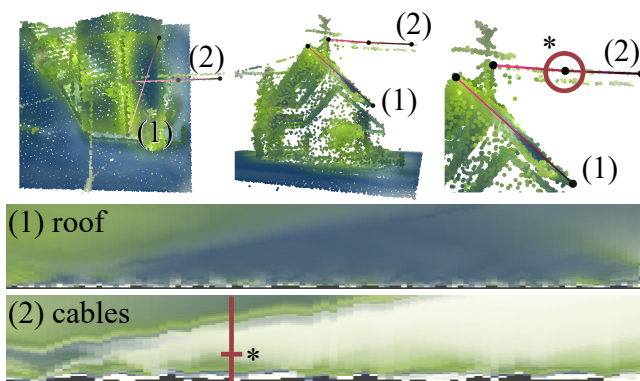


Figure 7: (Top:) Two line probes placed in real-world data. (1) on a roof, (2) along a cable bundle. (Bottom:) geometric multi-scale measures along the probes (left to right). Both exhibit low curvature, but yield different geometric classifications in the MSFIs.

5. Conclusion

We have proposed a visualization paradigm to illustrate and analyze local geometric features in point cloud neighborhoods. Features such as a geometric shape, indicating curvature or edges, and presence of noise become apparent in colored multi-scale feature images. Further, we examined the influence of radial weighting functions and the choice of a centroid on the geometric measures. The illustrations were utilized during the development of a line reconstruction algorithm, but may support other scale space based method developments. We compared to a curvature based scale space, which showed different properties related to geometric classification and contrast of regions in the images. As a further advantage, our approach also does not require normals. We presented the utilization in an analysis tool for light detection and ranging sensor data. In the future, we will improve the performance of the point cloud shape measures by GPU computing to maintain interactivity for large data. Also, we will explore geometric classification for clustering via the measures, to enhance the visualization. Finally, we will analyze a combination of the method of Mellado et al. [MGB*12] and ours, leveraging their advantages.

Acknowledgment: This research was funded through the Vice Rectorate of Research of the University of Innsbruck within the scope of the doctoral program *Computational Interdisciplinary Modelling (DK CIM)*.

References

- [AHK*13] AMIRKHANOV A., HEINZL C., KUHN C., KASTNER J., GRÖLLER M. E.: Fuzzy CT Metrology: Dimensional Measurements on Uncertain Data. In *SCCG 2013 - 29th Proceedings Spring conference on Computer Graphics* (2013), pp. 93–101. 1
- [CS20] CERVENKA M., SKALA V.: Behavioral study of various radial basis functions for approximation and interpolation purposes. In *IEEE 18th World Symp on Appl Mach Int and Inf (SAMI)* (2020), p. 135ff. 2
- [LCZ*18] LIN H., CHEN J., ZHANG Y., WANG W., KONG D.: Feature Preserving Filling of Holes on Point Sampled Surfaces Based on Tensor Voting. *Mathematical Problems in Engineering* (Aug 2018). 1
- [LMBM20] LEJEMBLE T., MURA C., BARTHE L., MELLADO N.: Persistence analysis of multi-scale planar structure graph in point clouds. *Computer Graphics Forum* 39 (2020), 35–50. 1
- [MGB*12] MELLADO N., GUENNEBAUD G., BARLA P., REUTER P., SCHLICK C.: Growing Least Squares for the Analysis of Manifolds in Scale-Space. *Computer Graphics Forum* 31 (2012), 1691–1701. 1, 3, 4
- [MGY*19] MO K., GUERRERO P., YI L., SU H., WONKA P., MITRA N. J., GUIBAS L. J.: Structurenet: Hierarchical graph networks for 3d shape generation. *ACM Trans. Graph.* 38, 6 (Nov. 2019). 1
- [MLGB20] MELLADO N., LEJEMBLE T., GUENNEBAUD G., BARLA P.: Ponca: a point cloud analysis library. <https://github.com/poncateam/ponca/>, 2020. 3
- [NBT10] NATALE D. J., BARAN M. S., TUTWILER R. L.: Point cloud processing strategies for noise filtering, structural segmentation, and meshing of ground-based 3d flash lidar images. In *2010 IEEE 39th Applied Imagery Pattern Recogn. Worksh. (AIPR)* (2010), pp. 1–8. 2
- [PKG03] PAULY M., KEISER R., GROSS M.: Multi-scale feature extraction on point-sampled surfaces. *Computer Graphics Forum* 22, 3 (2003), 281–289. 1
- [WLP*17] WEI M., LIANG L., PANG W.-M., WANG J., LI W., WU H.: Tensor Voting Guided Mesh Denoising. *IEEE Transactions on Automation Science and Engineering* 14, 2 (2017), 931–945. 1
- [WPG*97] WESTIN C., PELED S., GUDBJARTSSON H., KIKINIS R., JOLESZ F.: Geometrical diffusion measures for MRI from tensor basis analysis. In *Proc. of ISMRM, 5th Meeting, Canada* (1997), p. 1742. 2